different L/D ratios, and ϵ different pressures are necessary. Tracer runs at different gas consumption or gas generation rates are also needed.

8 Nomenclature

c	constant in equation for void fraction profile
C_L	liquid phase concentration, mol/cm^3
C_G	gas phase concentration, mol/cm^3
D_c	column diameter, m
D_L	liquid axial dispersion coefficient, cm^2/s
D_G	gas axial dispersion coefficient, cm^2/s
D_{rr}	radial turbulent diffusivity, cm^2/s
D_{zz}	axial turbulent diffusivity, cm^2/s
g	gravitational constant, cm/s^2
H	Henry's constant
K_La	overall liquid side volumetric mass transfer coefficient, cm/s
L	height of liquid dispersion, cm
m	void fraction exponent
U_G	superficial gas velocity, cm/s
$\bar{U}$	liquid circulation velocity, cm/s
z	axial position of detector, cm

Greek

α	fraction of Gas phase tracer detected
ϵ_G	gas holdup
$\tilde{\epsilon_G}$	constant in equation for void fraction profile
ρ	density, gm/cm^3
ψ	non dimensional radial position

Subscripts

G	gas
L	liquid
t	time

U	upflow regigion
z	axial posititon

9 References

Baird, M. H. and Rice, R. GG., 1975, Axial Dispersion in Large Unbaffled Columns. *Chem. Engng. J.*, **9**, 171-174.

Deckwer, W. D., Burchart, I R. and Zoll, G., 1974, Mixing and Mass Transfer in Tall Bubble Columns. *Chem. Engng. Sci.* **29**, 2177.

Degaleesan, S. and Dudukovvić, M. P., 1995, Experimental Quantification of Turbulence in Bubble Columns.s. Presented at the *AIChE Annual Meeting*, Miami Beach, Florida.

Degaleesan, S., Roy, S., Kunmar, S. B. and Duduković, M. P., 1996, Liquid Mixing Based on Convection and Turbulent Dispersion in Bubble Columns. *Chem.* Engng. Sci. **51**, 1967-1976.

Devanathan, N., Moslemian, D. and Duduković, M. P., 1990, Flow Mapping in Bubble Columns using CARPT. *Chem. Engng. Sci.* **45**, 2285-2291.

Devanathan, N., 1991, 'Investigation of Liquid Hydrodynamics in Bubble Columns via Computer Automated Radioactive Particle Tracking (CARPT)', D.Sc. Thesis, Washington University, St. Louis.

Field, R. W. and Davidson, , J. F., 1980, *Trans. Inst. Chem. Engrs.*, **58**, 228.

Hills, J. H., 1974, Radial Non-Uniformity of Velocity and Voidage in a Bubble Column. *Trans. Inst. Chem. Engrs.* **52**, 1-9.

Kato, Y., Nishiwaki, A., Fukuda, T. and Tanaka, S., 1972, *J. Chem. Eng. Japan*, **5**, 112.

Krishna, R., Wilkinson, P. M., and van Dierendonck, L. L., 1991, A Model for Gas Holdup in Bubble Columnns Incorporating the Influence of Gas Density on Flow Regime Transitions., *Chem. Engng. Sci.* **46**, 2491-2496.

Krishna, R., de Swart, J. W. A., Hennephof, D. E., Ellenberger, J. and Hoefsloot, H. C. J., 1994, Influence of Increased Gas Density on Hydrodynamics of Bubble-Column Reactors, *AIChE J.*, **40**, 112 - 119.

Kumar, S. B., Devanathann, N, Moslemian, D. and Duduković, M. P., 1994, Effect of Scale on Liquid Circulalation in Bubble Columns, *Chem. Engng. Sci.*, **49**, 5637-5652.

Kumar, S. B., Duduković, , M. P., Toseland, B. A. and Brown, D. M., 1996, Topical Report entitled 'Measuurement Techniques for Local and Global Fluid Dynamic Quantities in Two and l Three Phase Systems', for Contract DOE-FC 2295 PC 95051.

Mangartz, K. H. and Pilhaofer, T, 1980, *Verfahreustechnik*, **14**, 40.

Shollenberger, K. A. and OO'Hern, T. J., 1995, Report entitled ' Hydrodynamic Characterization of Slurry-PPhase Flow in the La Porte Alternative Fuels Development Unit (AFDU) using Difiifferential Pressure Measurements', Sandia National Laboratories.

Towell, G. D. and Ackermaan, G. H., 1972, Proceedings of the 5th European Symposium on Chemical Reaaction Engineering, B3-1, Elsevier, Amsterdam.

Tsoulfanidis, N, 1983, Meaasurement and Detection of Radiation, McGraw Hill, New York.

Wilkinson, P., M., 1991, PPhysical Aspects and Scale-up of High Pressure Bubble Columns, Ph.D. Thesisis, University of Groningen, Netherlands.

10 Appendix I: Holdup Measurements

This appendix deals with some of the aspects on holdup measurements, that were discussed in the main report. The differences in gas holdup estimates between the nuclear densitometer and γ ray tomography technique are shown in Figure A.1.1. In nuclear densitometry (left figure), the source emits a narrow beam of γ radiation through the column, with a detector opposite it. This yields a series of chordal measurements. A single line averaged holdup can be obtained across the centerline of the column. In γ ray tomography (CT), a series of scans is obtained at different angular positions to yield a distribution of void fraction across a given cross-section. The average holdups obtained from NDG are thus higher than the true cross-sectional average holdups from CT. More details are presented elsewhere (Kumar et al, 1995).

However, as the void fraction profile becomes more uniform , that is, with larger values for the void fraction exponent m in equation 14, the differences are reduced. This is illustrated in Figure A.1.2.

Figure A.1.3 (a) and (b) shows the axial holdup profiles in the column from DP and NDG measurements at various process rates.

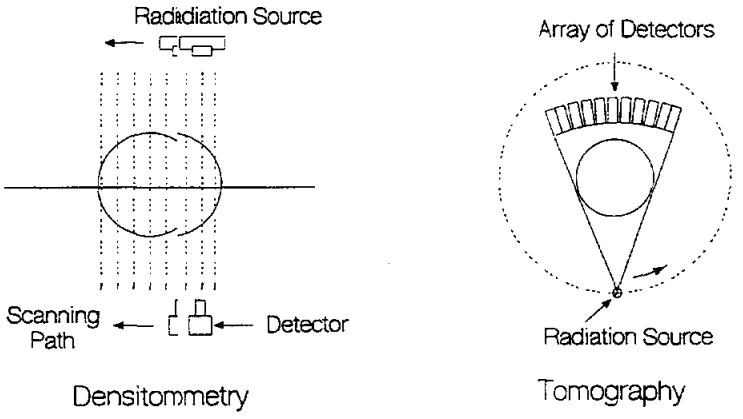

Figure A.1.1: Datata Collection for Densitometry and Tomography

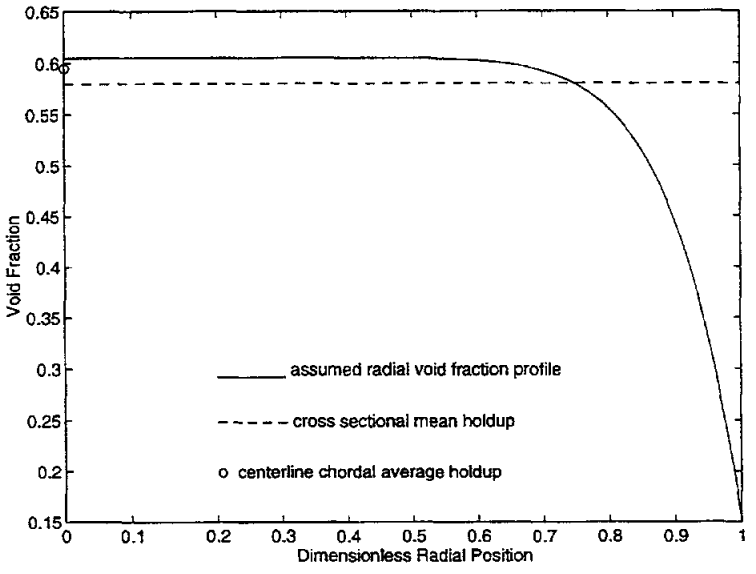

Figure A.1.2: Comparison of Assumed Void Fraction Distribution and Centerline Chordal Average

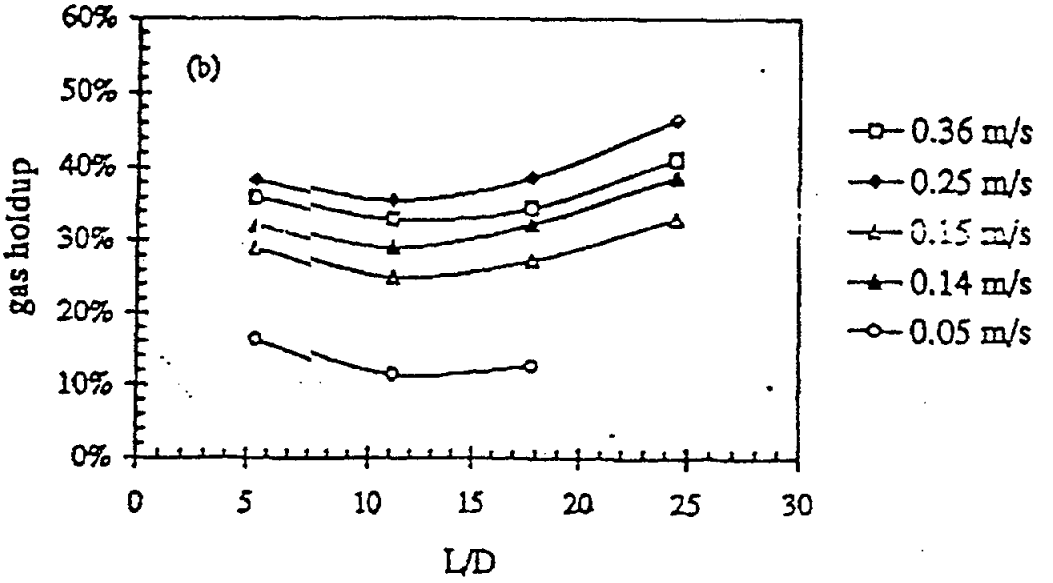

Figure A.1.3 (a) Axial Holdup Profile Measured by DP

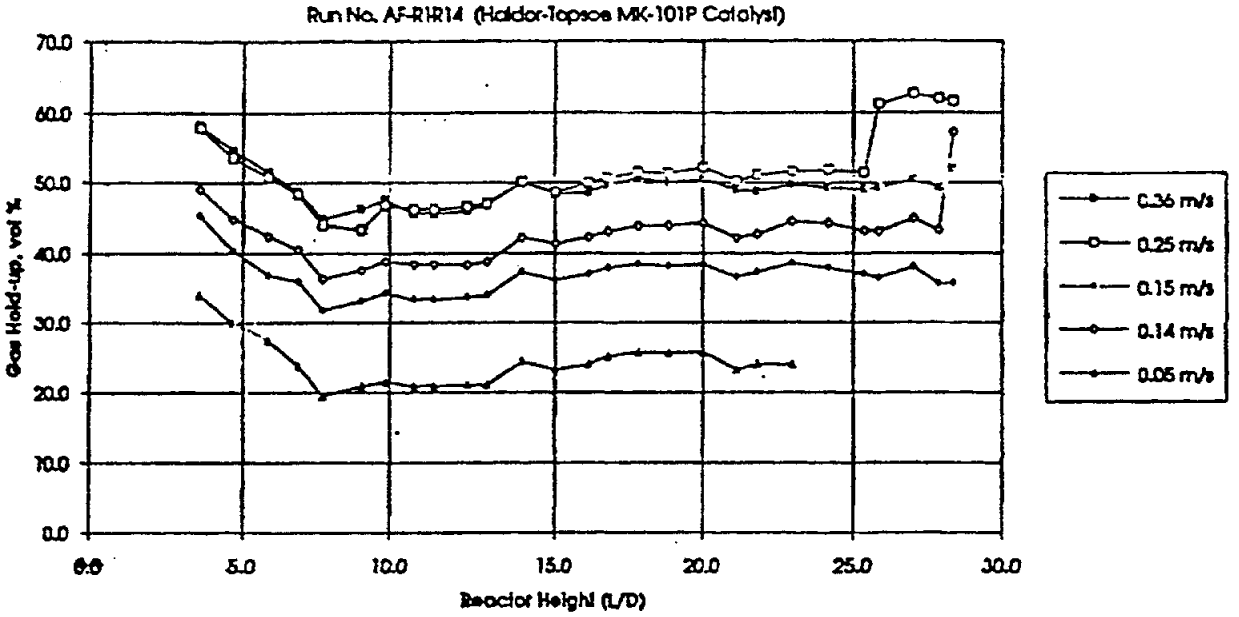

Figure A.1.3 (b) Axial Holdup Profile Measured by NDG

11 Appendix III: Simulation of the Radiation Intensity Meaasured by a Detector

The intensity of eadiatiicion from a point source recorded at a detector is given by the following expression:

$$n_p = AF.BF.\Omega.\eta.S \tag{24}$$

n_p is the count rate (countsts/time) at the detector due to a point source. Each factor is defined below.

The attenuation factor AFF is defined as

$$AAF = \exp[-(\mu_g l_g + \mu_{sl} l_{sl} + \mu_w l_w)] \tag{25}$$

in which μ_g, μ_{sl} and μ_w arare the linear attenuation coefficients in the gas, the slurry and the wall of the reactorr, and l_g, l_{sl} and l_w are the effective distances or depths of penetration in the respectitive media. The attenuation coefficient in the gas phase is negligible when compared i with the other phases, and so the term for the gas phase is ignored. l_{sl} takes into aaccount the liquid (slurry) holdup. The calculation of l_{sl} depends on the nature of t the holdup distribution. This assumes that the slurry is pseudohomogeneous. If thaat is not the case and if the attenuation coefficients for the solid and liquid are considderably different, then the term $\mu_{sl} l_{sl}$ must be replaced by $\mu_l l_l + \mu_s l_s$, where subscriptots s and l refer to solid and liquid, respectively.

The buildup factor BF reppresents the ratio of the intensity due to all photons to the intensity due to unscattereced photons alone. It is defined empirically using the Berger equation (Tsoulfanidis, 19883):

$$BF = 1 + (\ (a_{sl}\mu_{sl} l_{sl} + a_w \mu_w l_w)[\exp(b_{sl}\mu_{sl} l_{sl} + b_w \mu_w l_w)] \tag{26}$$

where a and b are the empppirical constants depending on the medium and energy of radiation.

The solid angle Ω is the frfraction of photons emitted by the source that is seen by the detector. For a shieldeled detector, only the front circular surface of the detector is exposed to the γ rays. FFor such a case, the solid angle is given by:

$$\Omega = \frac{1}{2}(1 - \cos(\tan^{-1}(R_c/d)) \tag{27}$$

where R_c is the radius of tlthe circular face of the detector, and d is the distance between the source and the c detector.

η, the efficiency of the detectctor, is taken to be a constant. S is the source strength. This is proportional to the cconcentration of tracer at a given location.

The detectors used are 2'2" x 2" NaI crystals, shielded on their sides. The various material constants at the eneergy levels of the source used are provided in Table A.2.1 (Tsoulfanidis, 1971).

Our objective is twofold. i. Initially we estimate the spatial range at a given axial position in the column over r which the detector receives its signal. The simulation is done for an assumed uniform n distribution of tracer and uniform distribution of phases. Secondly, we proceed to studdy the effect of the radially non-uniform gas holdup profile on the radiation received at t the detector

1. Uniform phase distributioon and concentration of tracer in gas and liquid phase

The medium is considereed to be homogeneous, with uniform phase and tracer distribution. Therefore the e effective distance in the liquid (slurry) medium used in Equation 25 and 26 is givenn as

$$l_{sl} = l_{sd}(1 - \epsilon_G) \tag{28}$$

where l_{sd} is the distance betwtween the source and center of the detector. The source strength or local activity is tlthe same at all locations, since the concentration of tracer (which is proportional to the e local source strength) is uniform. Substituting for all the factors into Equation 24, the e count rate recorded at the detector due to the individual uniformly distributed point s sources is calculated. The resulting spatial distribution of intensity (counts/time) atat a given axial position is shown in Figure A.2.1. The position of the detector relatitive to the intensity distribution is shown in Figure A.2.2. The perpendicular distance bbetween the face of the detector and the wall of the column is 2.54 cm (1 inch). The shaaded region in Figure A.2.2. represents the volume (area) considered for the contributition of the radiation to the overall radiation received at the detector. The total radiaiation from this shaded region, which forms less than 1 % of the entire reactor volume.e, is 90 % of the total radiation from the entire domain. Since the detector is shieldeedd on its sides, the contribution of radiation from different axial positions other than tlthe cross-sectional slice (10 cm in thickness) at the axial position of the detector is neaegligible. Therefore it can be assumed that the radiation

measured at the detector atat a given axial position is proportional to the concentration of tracer at that axial locatation.

2. Uniform tracer concentrtration and variable gas holdup profile

It is well known that tlthere exists a cross-sectional holdup profile in the column. The effect of this profile, that is, variation in holdup, can be accounted for in the simulation of the radiationn measured at the detector. This is done as follows:

- The gas phase modelel is used to estimate the cross-sectional average gas and liquid tracer concentrtrations (C_G and C_L) at a given axial location and time.
- A suitable radial holddup profile of the gas $\epsilon_G(r)$ and thereby the liquid $\epsilon_L(r)$ is assumed (Kumar, 19994).
- The attenuation factctor (AF) and buildup factor BF are calculated by accounting for the local variaiation in the phase distribution.

$$AFF = \exp(-([\int_{p_0}^{p_d} \mu_{sl}(1 - \epsilon_G(r))dl] + \mu_w l_w)) \tag{29}$$

where p_0 and p_d derenote the position of the source and detector. A similar expression is used fonr the buildup factor, which takes into account the varying phase distribution. TThereby the effects of radial gas holdup profile are properly accounted for in the factors AF and BF. The solid angle and efficiency remain unchanged from the previously discussed values. The source strength at a given point in the cross-secctional plane is calculated as

$$SS(r, z, t) = \epsilon_G(r)C_G(t, z) + \epsilon_L(r)C_L(t, z) \tag{30}$$

Substituting for the individual factors into Equation 24 and integrating over the filed of view of thhe detector, the overall count rate is calculated, which gives the total tracer concecentration at a given axial location $C_t(t, z)$.

In this simulation, the gas profile given by equation 21 is used with an exponent of $m = 3$. The effect of gas aand liquid tracer concentration on the resultant count rate at the detector is shown iiin Figure A.2.3.(a), (b) and (c). When the gas and liquid tracer concentration are eequal, the simulated profile is steep, similar to Figure A.2.1 with a sharp exponential decay. However, as the concentration of liquid tracer is

reduced, the profiles become flatter, and the contribution of the tracer in the shaded region of Figure A.2.2. to thee total radiation is reduced (Fig A.2.3.(c)).

Therefore when the concentration of tracer in the liquid phase is low enough, as in the present situation, the (cross-sectional) spatial contribution of radiation from the tracer at a given axial location becomes uniform and the simplified expression for C_t given by Eqn 7 is valid.

Table A.2.11 : Constants for Radiation Simulation

$\mu_{sl\,sl}$	0.065 cm^{-1}	μ_w	0.40 cm^{-1}
$a_{sl\,sl}$	1.4	a_w	1.27
$b_{sl\,sl}$	0.027	b_w	0.032

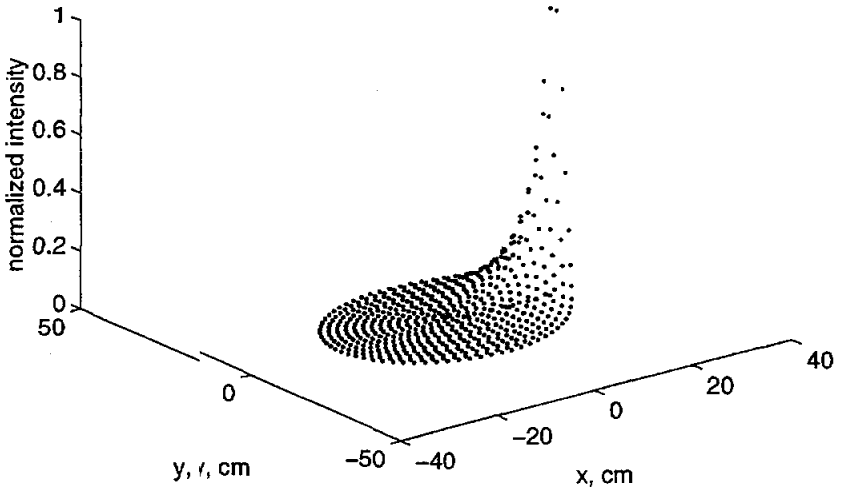

Figure A.2.1: (a) Three-Dimensional riew of the (x,y) Spatial Distribution of Intensity in a Cross-Sectional Slice of the Reactor. Each '.' denotes a discrete source point at an (x,y) location.. Position of detector is shown in Fig. A.2.2. Contribution of the shaded region in Figig. A.2.2. is 90 %.

cm

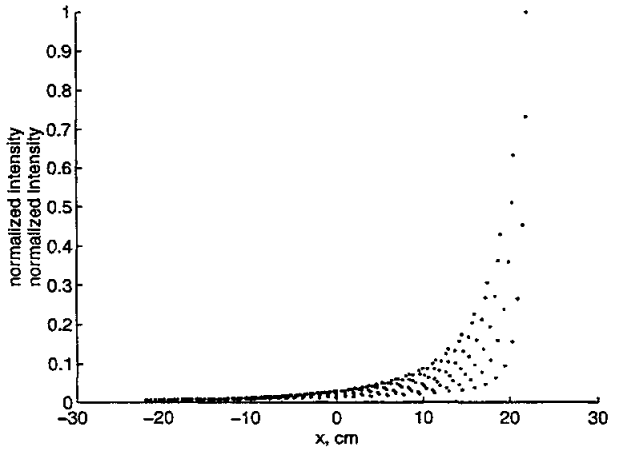

Figure A.2.1: ı (b) Front View (along x-axis) of Fig. A.2.1(a)

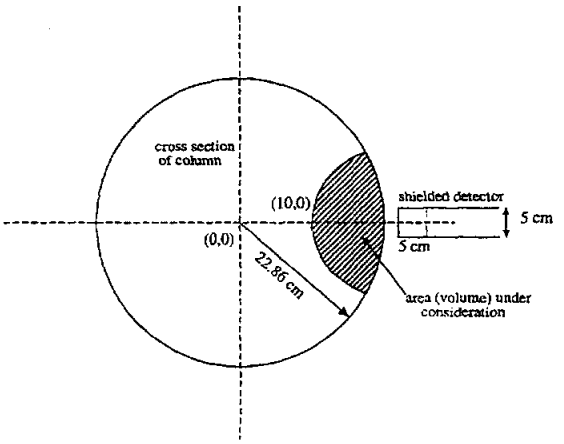

Figure A.2.2: Cross sectionalal view of the column with detector positioned along the 'x' axis. Shaded region repre:esents the region considered for the contribution of radiation to the overall radiaiation received by detector.

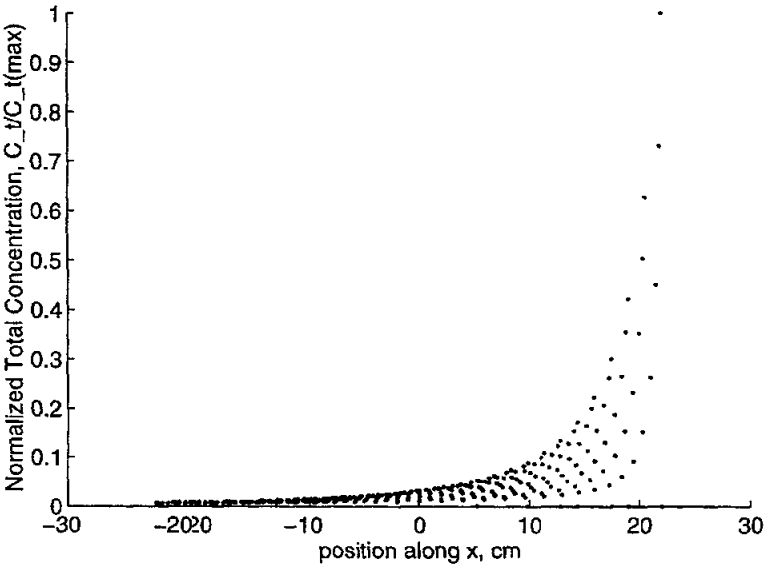

Figure A.2.3: (a) Front Vieww of the (x,y) Spatial Distribution of Radiation with Non-Uniform Gas Holdup, aand Equal Gas and Liquid Phase Tracer Concentration. The contribution of the shadded region in Fig. A.2.2. to the total radiation detected is 88 %.

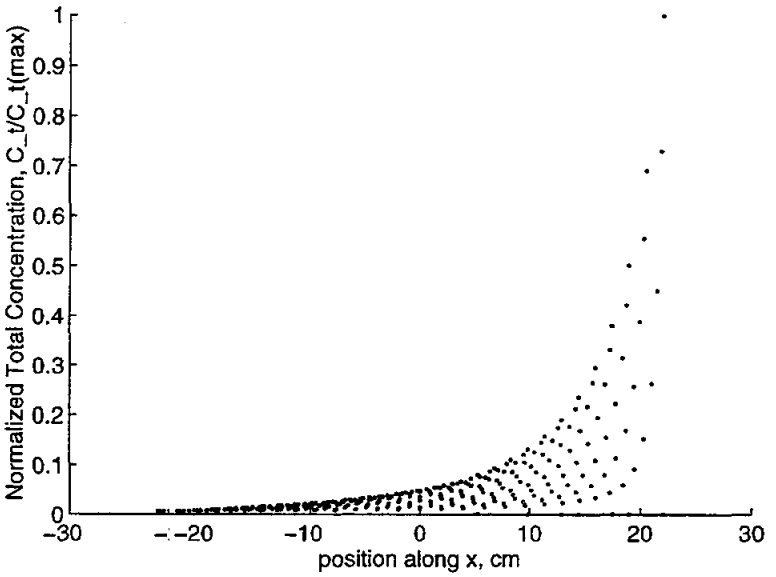

Figure A.2.3: (b) Front Viiew of the (x,y) Spatial Distribution of Radiation with Non-Uniform Gas Holdup, , and Ratio of Gas and Liquid Phase Tracer Concentration 1:0.5. The contribution of f the shaded region in Fig. A.2.2. to the total radiation detected is 79 %.

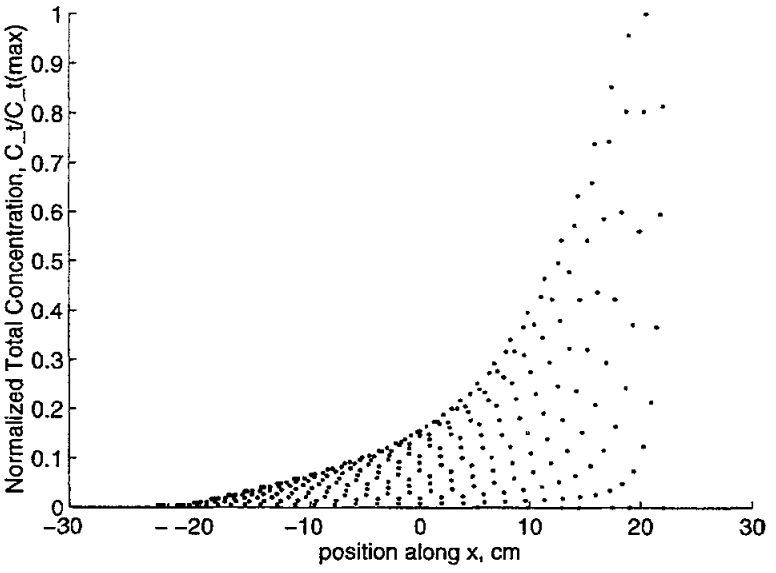

Figure A.2.3: (c) Front vieew of the (x,y) spatial distribution of radiation with non uniform gas holdup, and raratio of gas and liquid phase tracer concentration 1:0.1. The contribution of the shnaded region in Fig. A.2.2. to the total radiation detected is 61%.

12 Appendix IIII: Liquid Tracer Experiments and Model Fits

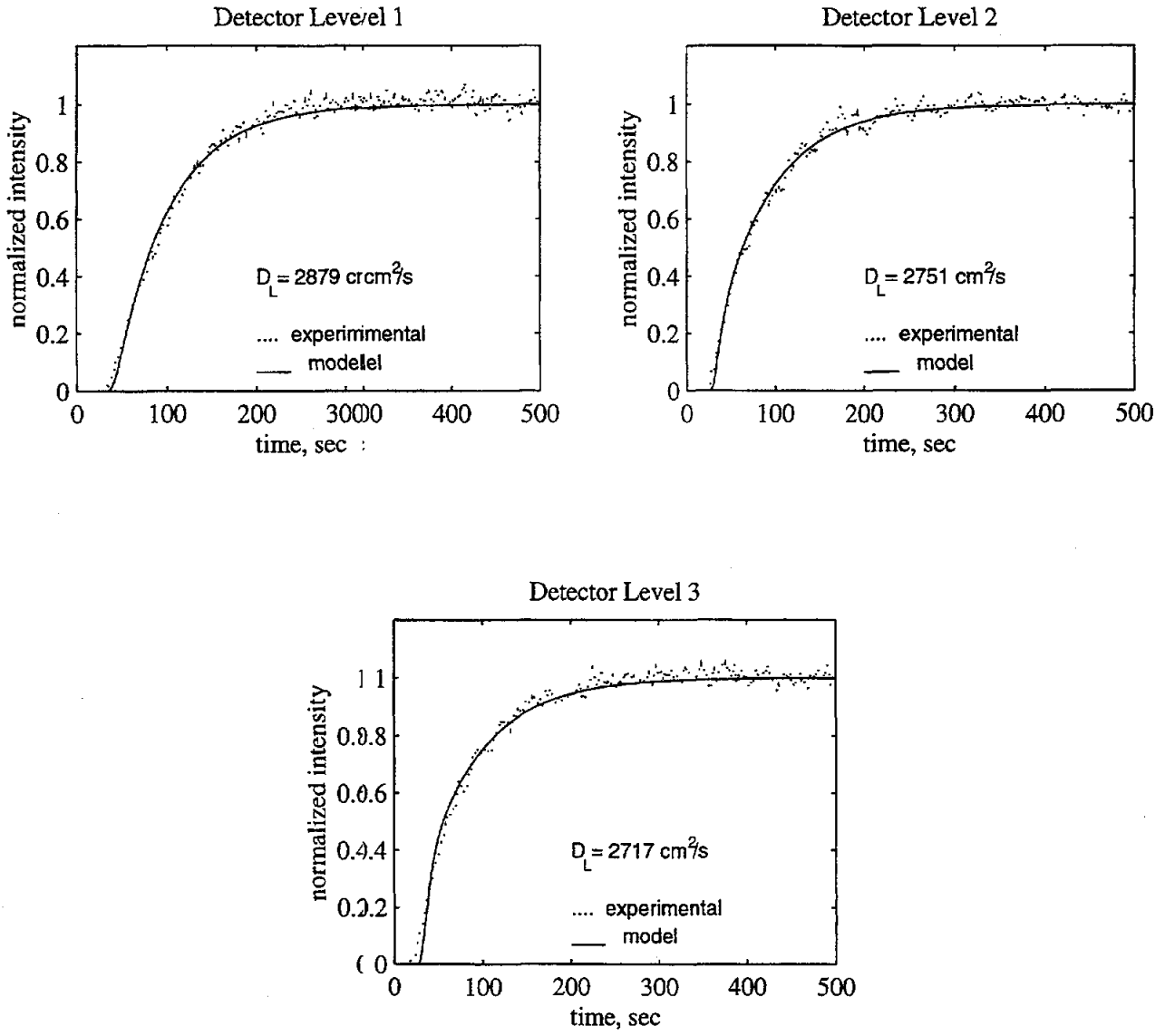

Figure A.3.1: Liquid Impulsse Response Mesurements for Run 14.6, N1-CEN, (5.2 MPa, U_G = 25 cm/s), Injectition Time 7.2s

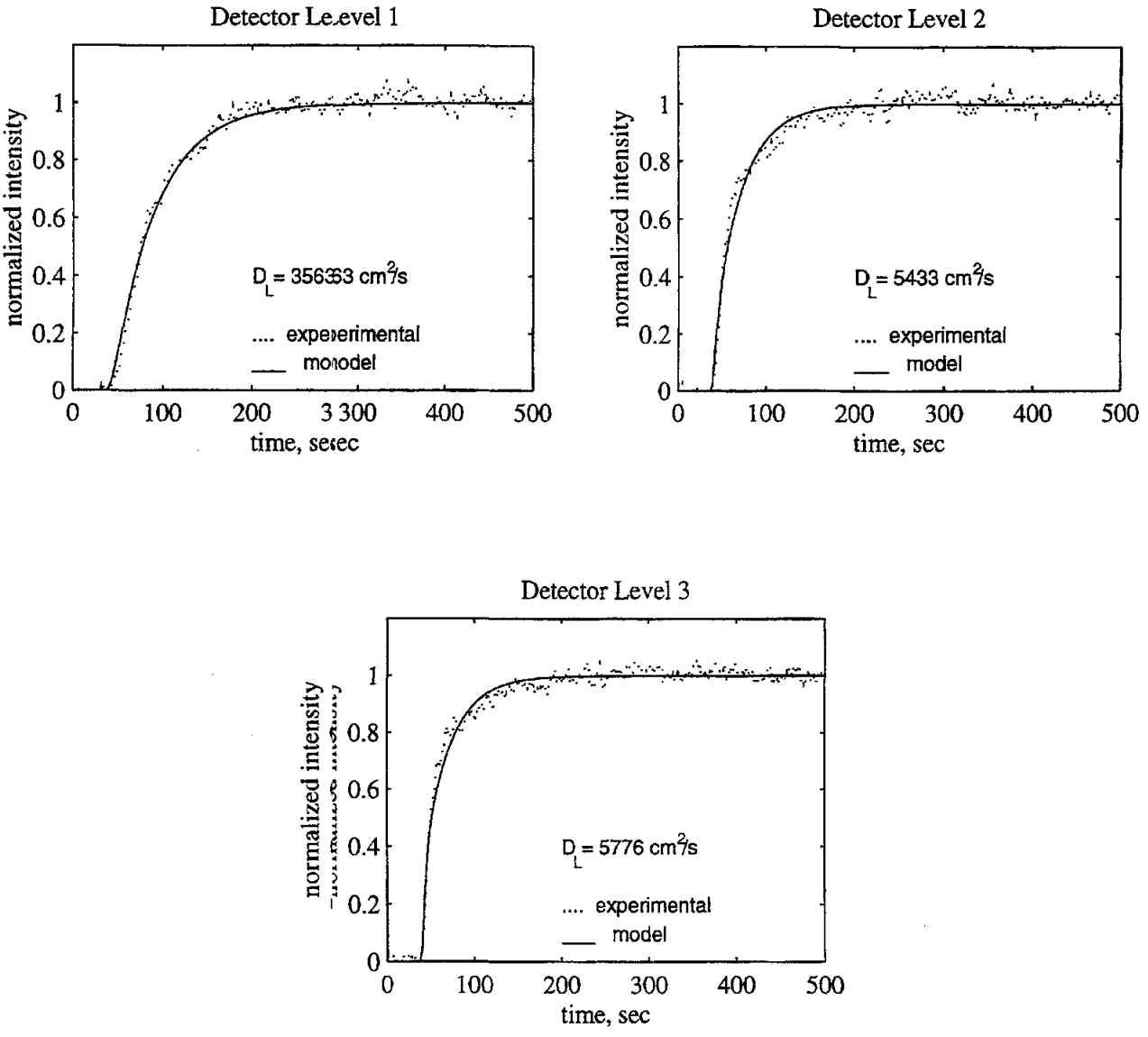

Figure A.3.2: Liquid Impululse Response Mesurements for Run 14.6, N1-WALL, (5.2 MPa, U_G = 25 cm/s), Injection Time 30.8s

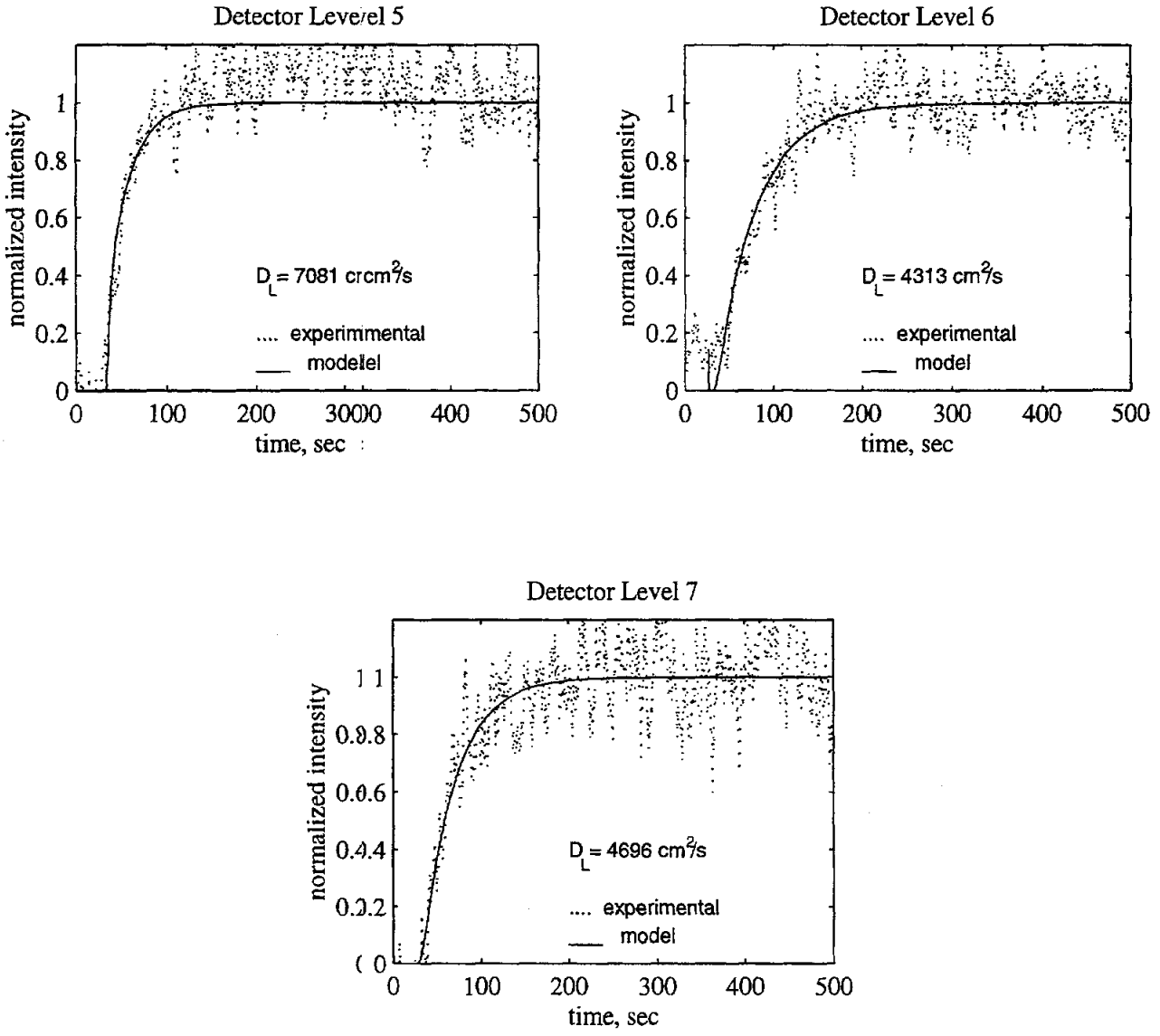

Figure A.3.3: Liquid Impulsse Response Mesurements for Run 14.6, N2-CEN, (5.2 MPa, U_G = 25 cm/s), Injectition Time 16.2s

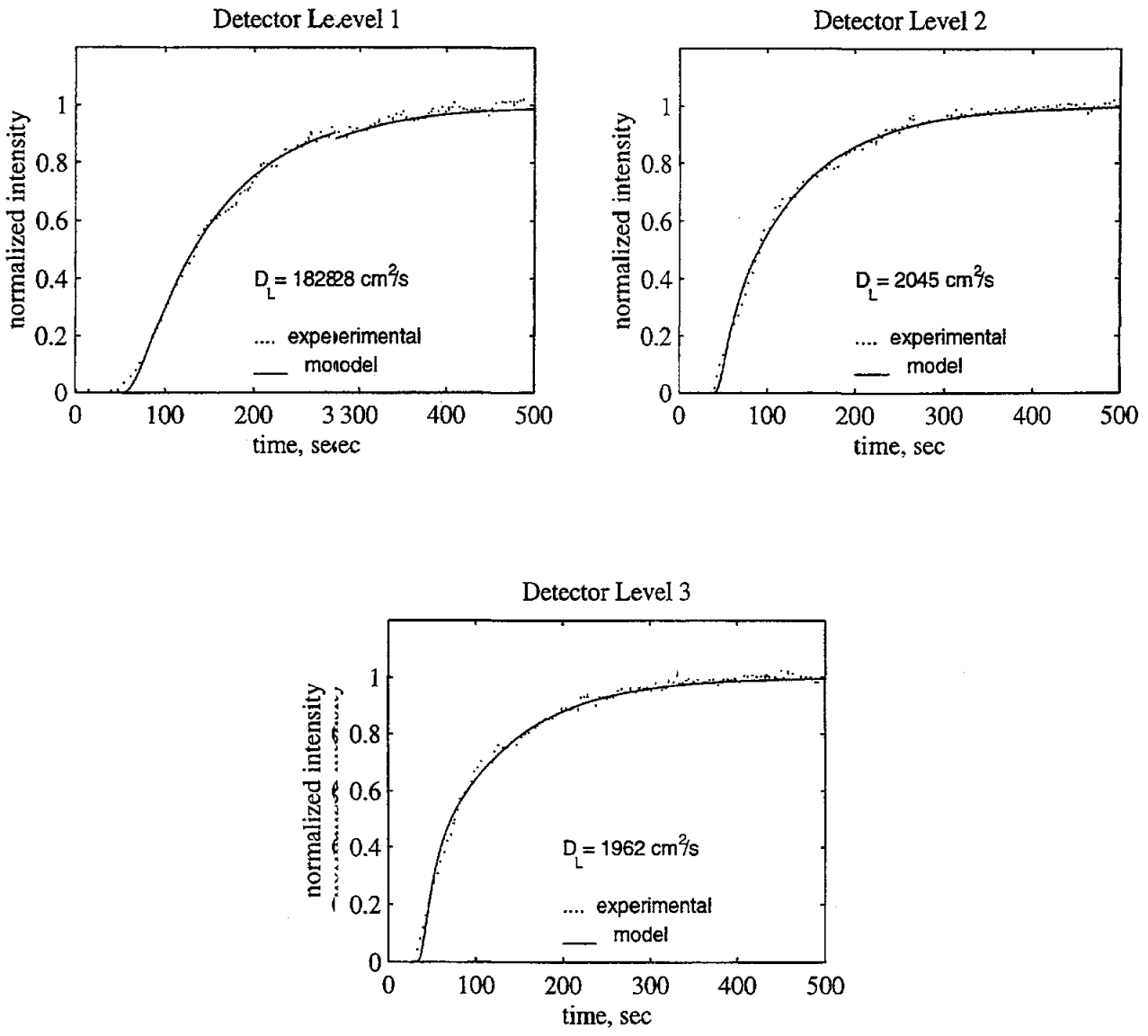

Figure A.3.4: Liquid Impululse Response Mesurements for Run 14.7, N1-CEN, (5.2 MPa, $U_G = 14$ cm/s), Injeection Time 26.4s

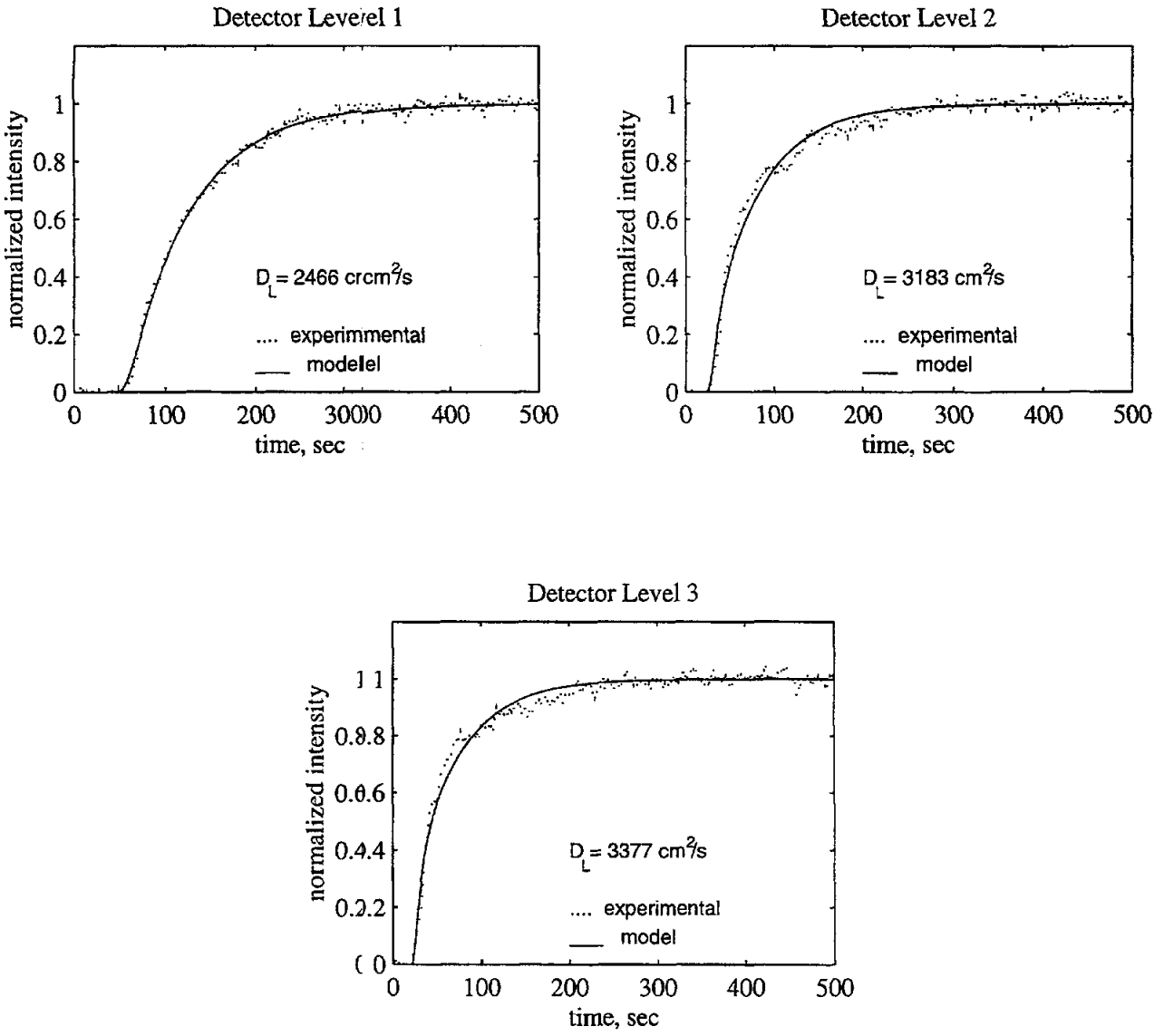

Figure A.3.5: Liquid Impulsse Response Mesurements for Run 14.7, N1-WALL, (5.2 MPa, U_G = 14 cm/s), Injectition Time 25.5s

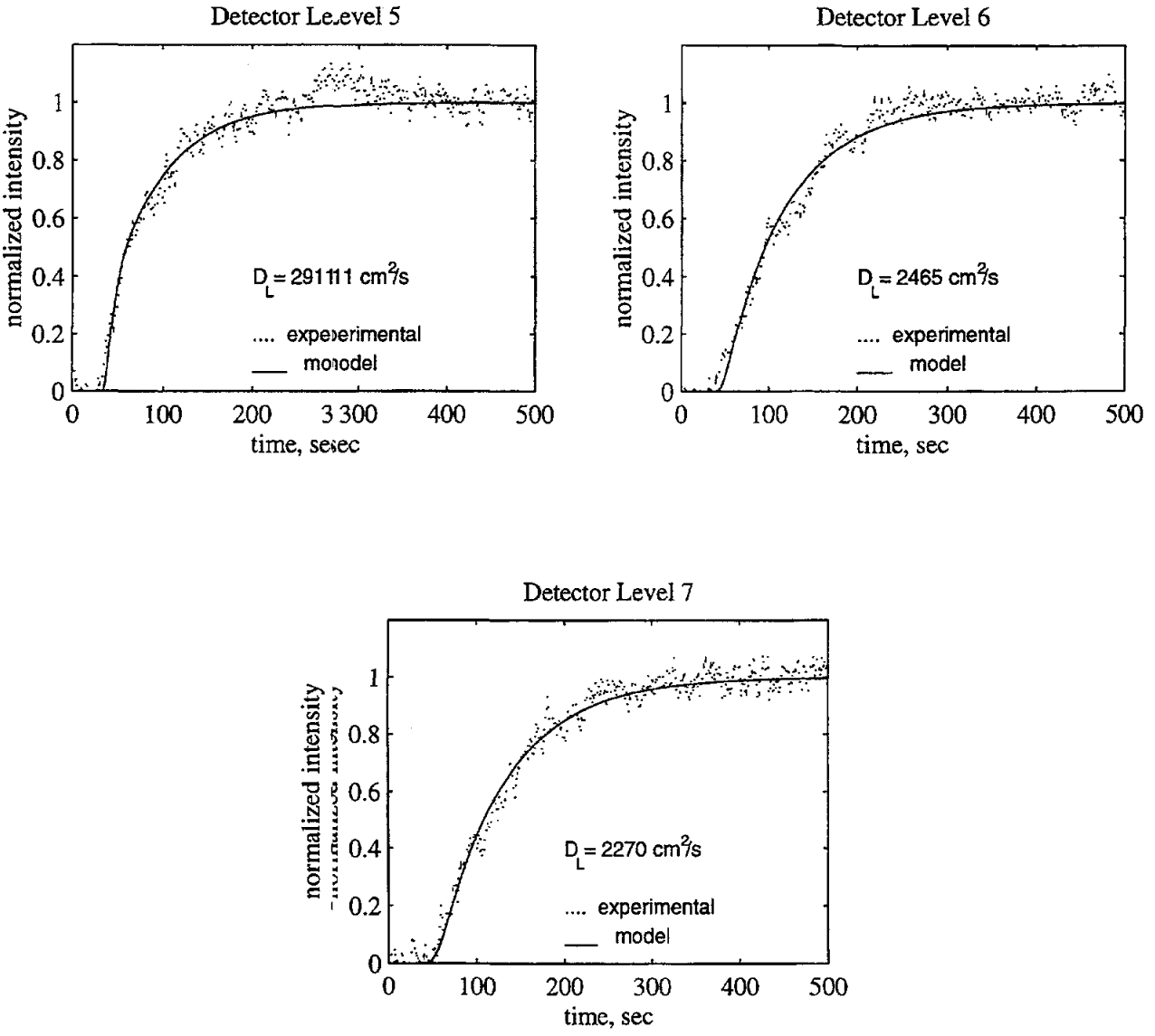

Figure A.3.6: Liquid Impulse Response Mesurements for Run 14.7, N2-WALL, (5.2 MPa, U_G = 14 cm/s), Injection Time 9.8s